27°). It is seen that the influence of crossflow on the radiative-flux ratio q/q_a is not large when expressed as a function of the radiation-cooling parameter Γ. Note, however, that the value of Γ is dependent on the crossflow, being linearly related to the crossflow factor F.

The result of Eq. (9) for F may be improved upon by consideration of two alternative approximations for the flow structure. The streamline pattern may be estimated, if it is assumed that the velocity component u_ϕ is time-invariant. In this case, the following equation is used in place of Eq. (4):

$$dt = dS/u_c = (S \sin\theta \, d\phi)/[u_\phi(\phi_t)] \tag{23}$$

With Eq. (23), the expression for F can be shown to be

$$F = (2/C)e^{2/C}[-Ei(-2/C)] \tag{24}$$

where $-Ei(-x)$ is the exponential integral defined by

$$-Ei(-x) = \int_x^\infty \frac{e^{-\xi}}{\xi} d\xi > 0 \qquad \infty > x > 0$$

A final flow approximation is that the velocity component u_ϕ is uniform across the shock layer with $u_\phi = u_\phi(\phi)$. In this case,

$$dt = dS/u_c = (S \sin\theta \, d\phi)/[u_\phi(\phi)] \tag{25}$$

The corresponding expression for F can be shown to be

$$F = 2/(2 + C) \tag{26}$$

The three expressions of F are compared in Fig. 3. The spread of the curves is not large. When the ϕ pressure gradient is taken into account, the F curve is expected to fall between the two curves marked "time-invariant u_ϕ" and "uniform u_ϕ." Therefore, it may be adequate to use the F curve marked "time-invariant u_ϕ" (or Eq. 24) for calculation of the adiabatic shock-layer thickness Δ_a, adiabatic radiation flux q_a, and, hence, the energy loss parameter Γ. As shown by the comparison of Fig. 2, the relatively simple formula of Eq. (22) (or Fig. 2 of Ref. 1) may be used as a good engineering approximation in evaluation of q/q_a.

References

[1] Chin, J. H. and Hearne, L. F., "Shock-layer radiation for sphere-cones with radiative decay," AIAA J. 2, 1345–1347 (1964).

[2] Hayes, W. D. and Probstein, R. F., *Hypersonic Flow Theory* (Academic Press, New York, 1959), p. 146.

Stagnation-Point Heat Transfer and Shock-Detachment Distance for Ellipsoids of Revolution

E. J. Felderman* and R. C. Fellinger†
Iowa State University, Ames, Iowa

Nomenclature

a = axis of capping ellipse measured perpendicular to body axis
b = axis of capping ellipse measured along body axis
h = enthalpy
h_D = enthalpy of dissociation
Le = Lewis number
M_s = Mach number of initial shock wave in shock tube
P_1 = initial channel pressure in shock tube
Pr = Prandtl number
q = stagnation-point heat-transfer rate

Received February 18, 1965.

* Department of Mechanical Engineering. Student Member AIAA.

† Professor of Mechanical Engineering.

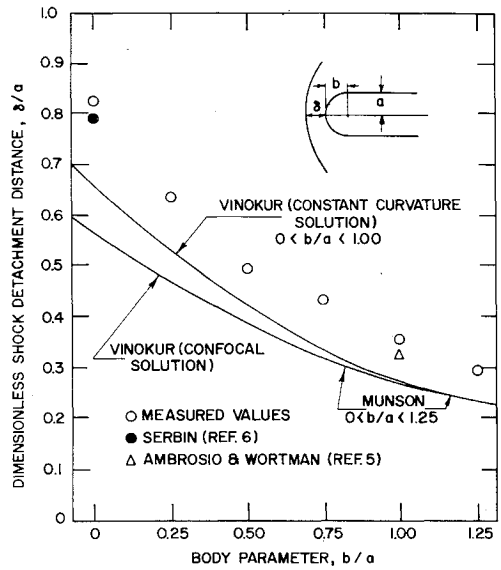

Fig. 1 Dimensionless shock-detachment distance as a function of body parameter, M_s = 5.12, P_1 = 5.25-mm Hg.

q_h = theoretical stagnation-point heat-transfer rate for a hemisphere
u_e = velocity component parallel to body surface
x = distance measured along body surface from stagnation point
δ = shock-detachment distance
μ = viscosity
ρ = density

Subscripts

s = stagnation conditions
w = wall conditions

Introduction

CONSIDERABLE stagnation-point, heat-transfer, and shock-detachment data have been reported in the literature for basic shapes, such as the hemisphere cylinder and the flat-faced cylinder. It would seem desirable to have additional data to bridge the gap between these shapes. The purpose of this investigation is to obtain such data for a series of blunt bodies formed by cylindrical afterbodies capped by ellipsoids of revolution. The bodies are characterized by the ratio b/a of the axis of the ellipse along the body axis to the axis perpendicular to the body axis as shown in Fig. 1. The values of the parameter b/a selected for the six models were: 0(flat-faced), 0.25, 0.50, 0.75, 1.00 (hemisphere), and 1.25. The experimentally measured stagnation-point heat-transfer rates and shock-detachment distances were compared with existing theoretical results. The theoretical analysis has been separated into an inviscid analysis of the flow field external to the boundary layer and a viscous boundary-layer analysis.

Boundary-Layer Analysis

A solution for the viscous boundary-layer valid near the stagnation point has been obtained by Fay and Riddell.[1] They wrote the boundary-layer equations including the effects of dissociation and ionization and obtained solutions by numerical methods. Fay and Riddell present the following correlation equation for stagnation-point heat transfer through an equilibrium boundary layer:

$$q = 0.76\, Pr^{-0.6}(\rho_s\mu_s)^{0.4}(\rho_w\mu_w)^{0.1}(h_s - h_w)(du_e/dx)^{0.5} \times [1 + (Le^{0.52} - 1)h_D/h_s] \tag{1}$$

The only term in this equation that depends on the flow field external to the boundary layer is the stagnation-point velocity gradient du_e/dx.

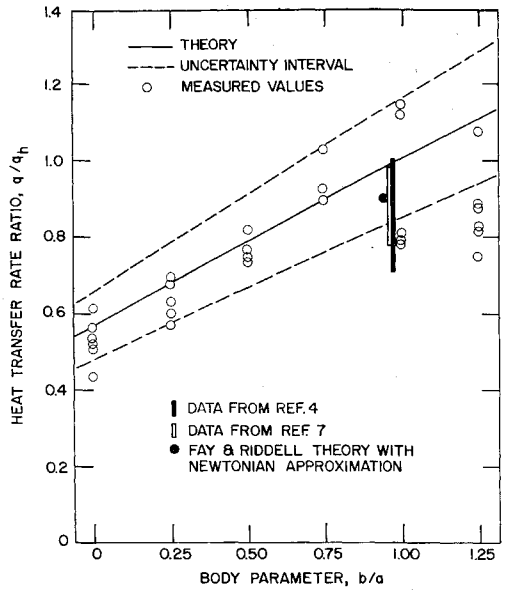

Fig. 2 Stagnation-point heat-transfer rate ratio as a function of body parameter, $M_s = 5.12$, $P_1 = 5.25$-mm Hg.

Inviscid Flow-Field Theory

A number of methods have been used to predict the inviscid flow field about a blunt body. For a hemisphere, the Newtonian approximation has been shown to give a good prediction for the stagnation-point velocity gradient. However, for bodies other than the hemisphere the Newtonian approach is unsatisfactory. The most exact approach is to solve the inviscid flow equations by means of numerical integration. A disadvantage of this method is that a numerical solution must be carried out for every flow condition. In order to obtain a simpler solution, several investigators have assumed the flow field between the detached shock wave and the boundary layer to be of constant density. Vinokur[2] used this approach to obtain a solution for oblate ellipsoidal shock waves, and Munson[3] extended it to both oblate and prolate ellipsoids. With this method, the shock wave and the generating body are found to be of the same shape. These authors present calculated values for both the stagnation-point velocity gradient and the shock-detachment distance as a function of the density ratio across the detached shock wave. Stagnation-point heat-transfer rates were calculated with the Fay and Riddell equation using these values for the velocity gradient.

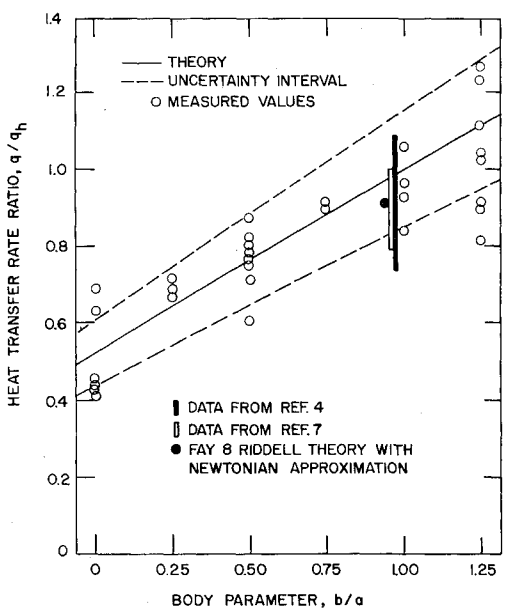

Fig. 3 Stagnation-point heat-transfer rate ratio as a function of body parameter, $M_s = 6.27$, $P_1 = 1.25$-mm Hg.

Equipment and Data Reduction

The experimental results of this investigation were obtained with the Iowa State University shock tube, which has a 3- by 6-in. constant area channel section 35 ft in length. Flow properties were calculated from measured values of initial shock speed, channel pressure, and temperature, using equilibrium air tables. For this series of tests both the driver gas, helium, and the driven gas, air, were at an initial temperature of 540°R. Shock-detachment distances were measured from schlieren photographs.

Thin platinum film heat-transfer gages, which have been used extensively,[4] were mounted at the stagnation point of each of the models to measure the surface temperature. The heat-transfer rate can be derived from the surface temperature-time history if the model is assumed to act as a semi-infinite body. The resulting expression was numerically evaluated using the Iowa State University Cyclone digital computer.

Discussion of Experimental Results

Shock-detachment distances were measured at shock-tube conditions of an initial shock-wave Mach number of 5.12 and an initial channel pressure of 5.25-mm Hg absolute. The shock-detachment distance was made dimensionless by dividing it by the afterbody radius. The dimensionless ratio is plotted as a function of body parameter in Fig. 1. The measured values for the hemisphere cylinder and the flat-faced cylinder are seen to agree within 7% with the results reported by Ambrosio and Wortman[5] and Serbin.[6] One solution of Vinokur[2] assumes that the shock wave is an ellipsoid confocal with the body, whereas the other assumes that the shock wave is of constant curvature in the region of the axis. The solution presented by Munson[3] yields the same result as the confocal solution of Vinokur. It is evident from Fig. 1 that the constant-curvature solution gives the best prediction of shock-detachment distance for this flow condition. Although the predicted values are approximately 20% low, the trend with body parameter is clearly indicated.

The stagnation-point heat-transfer rates shown in Figs. and 3 are made dimensionless by dividing them by the stagnation-point heat-transfer rate for a hemisphere computed with the theory of Fay and Riddell used in conjunction with the constant-curvature solution of Vinokur. This rate was 257 Btu/ft² sec in Fig. 2 and 246 Btu/ft² sec in Fig. 3. Stagnation-point heat-transfer rates were measured on the six models at two flow conditions. In Fig. 2 the stagnation-point heat-transfer rate ratio is plotted as a function of the body parameter b/a for a shock-tube flow condition of an initial shock Mach number of 5.12 and an initial channel pressure of 5.25-mm Hg absolute. In Fig. 3, the flow condition was an initial shock Mach number of 6.27 and an initial channel pressure of 1.25-mm Hg absolute. The theory line shown in Figs. 2 and 3 is computed from the theory of Fay and Riddell in conjunction with the constant-curvature solution of Vinokur for the velocity gradient. The theory line is seen to be approximately 10% high when compared with the shock-tube data for the hemisphere from Refs. 4 and 7. A point computed from the Fay and Riddell theory with a Newtonian approximation for the velocity gradient is also shown for the hemisphere. The majority of the data fall within a band of ±15.5%, obtained from an error analysis, which is shown attached to the theory line. Although there is considerable scatter in the data, the trend with body parameter is evident. In view of this, it is felt that the theories used are sufficiently accurate for approximate engineering calculations. It is felt that the data presented help bridge the gap between the basic shapes represented by the hemisphere cylinder and the flat-faced cylinder.

References

[1] Fay, J. A. and Riddell, F. R., "Theory of stagnation point heat transfer in dissociated air," J. Aeronaut. Sci. **25**, 73–85 (1958).

[2] Vinokur, M., "Hypersonic flow around bodies of revolution which are generated by conic sections," Proc. Midwestern Conf. Fluid Mech. 6, 232–253 (1959).

[3] Munson, A. G., "Constant density approximations for the flow behind axisymmetric shock waves," NASA TN D-857 (1961).

[4] Rose, P. H. and Stark, W. I., "Stagnation point heat transfer measurements in air at high temperature," Avco Research Lab. Research Note 24 (1956).

[5] Ambrosio, A. and Wortman, A., "Stagnation-point shock-detachment distance for flow around spheres and cylinders in air," J. Aerospace Sci. **29**, 875 (1962).

[6] Serbin, H., "Supersonic flow around blunt bodies," J. Aeronaut. Sci. **25**, 58–59 (1958).

[7] Ross, P. A., "Shock tube data report on stagnation point heat transfer in air," Boeing Co. Rept. D2-22007-1(1963).

Dynamic Efficiency of Pulsed Plasma Accelerators

Neville A. Black* and Robert G. Jahn†

Princeton University, Princeton, N. J.

In most pulsed plasma accelerators, such as coaxial guns, pinch engines, T-tubes, etc., the essential magnetogasdynamic interaction is the acceleration of a current-carrying region of plasma by its own magnetic field into an ambient body of gas. The piston action of this accelerated current zone in turn generates a strong shock wave that propagates slightly ahead of it and serves to compress the ambient gas as well as accelerate it to the piston velocity. It is well known that such strong shock waves propagating at constant velocity into gases at rest convert about 50% of the available energy into organized streaming motion of the shocked gas and 50% into its internal, i.e., random thermal, energy. This property has on occasion been invoked as a criterion for the limiting performance of such accelerators. For example, Larson et al.[1] have contended that, in the range of shock strengths prevalent in useful pulsed plasma thrustors, the specific enthalpy of the shocked gas is so high that the bulk of its internal energy will be lost by radiation before it can be recovered by expansion at the orifice. Thus, they suggest, such thrustors may labor under an intrinsic 50% efficiency limitation.

This criterion seems excessively severe. On the one hand there is certain experimental evidence that the internal equilibration and radiation processes are not sufficiently rapid to dispose of the bulk of the internal energy on the time scale involved.[2] But, even conceding no recovery of internal energy for useful thrust work, the 50% criterion pertains only to special gasdynamic situations, such as the quoted case of constant velocity propagation into ambient gas at rest. Guman,[3] for example, has shown that a prior streaming motion of the ambient gas fill substantially alters the energy division for constant shock propagation velocity. It is the purpose of this note to display a simple analytical argument whereby the energy division can be estimated for arbitrary profiles of shock velocity along the accelerator channel as well as for arbitrary one-dimensional accelerator geometries and initial gas density distributions.

Received March 8, 1965.

* Graduate Student, Department of Aerospace and Mechanical Sciences. Member AIAA.

† Associate Professor, Department of Aerospace and Mechanical Sciences. Associate Fellow Member AIAA.

Consider the conventional snowplow idealization of the process,[4] wherein a thin current sheet is driven by its own magnetic field into a gas at rest and accumulates within a negligibly narrow region on its surface all of the gas that it overtakes. Starting from a simple Newtonian statement of the over-all dynamics of the situation, one can identify two components of the rate of energy deposition

$$vF = v(d/dt)(mv) = (d/dt)(\tfrac{1}{2}mv^2) + (v^2/2)(dm/dt) \quad (1)$$

where F is the instantaneous driving force, m the mass accumulated on the piston, and v its velocity. The first term on the right is the rate of increase of streaming kinetic energy of the swept gas immediately useful for propulsion. The second term represents the dissipation associated with the inelastic collision of the incoming particles with the snowplow piston. (The rigorous validity of this representation for the actual gasdynamic acceleration process behind a strong shock wave is a rather subtle point developed in detail elsewhere.[5])

Imagine that the preceding process starts with some initial velocity v_0 and continues over a period of time t_f, at the end of which the piston has progressed a distance x_f and has accumulated a total mass m_f, which is now moving at a velocity v_f. The ratio of interest is that of the integrals of the foregoing two terms over this period:

$$\alpha = \left(\int_0^{t_f} \frac{v^2}{2}\frac{dm}{dt}\,dt\right)\Big/\left(\frac{1}{2}m_f v_f^2\right) \quad (2)$$

which determines the dynamic efficiency of the process

$$\eta = 1/(1 + \alpha) \quad (3)$$

At this point it might be noted that, in the very special case where the piston begins its motion with the total mass to be accelerated already entrained ("slug" model), dm/dt will be zero thereafter, and the efficiency η will be in identical unity.

Returning to the general problem, we convert to dimensionless distance, velocity, mass, and time variables:

$$X = x/x_f \qquad V = v/v_0 \qquad M = m/m_f$$
$$T = tv_0/x_f \quad (4)$$

The geometry of a specific accelerator and the ambient gas density distribution are embodied in the functional dependence of accumulated mass on piston position

$$M = \mu(X) \quad (5)$$

In terms of these dimensionless quantities, the energy-division ratio α becomes

$$\alpha = \left[\int_0^{T_f}\left(\frac{dX}{dT}\right)^3\frac{d\mu}{dX}\,dT\right]\Big/\left(\frac{dX}{dT}\right)_f^2 = \left[\int_0^1 V^2\frac{d\mu}{dX}\,dX\right]\Big/V_f^2 \quad (6)$$

In general, the development of the dimensionless velocity profile $V(X)$ is determined by the magnitude and waveform of the discharge current as well as by the geometry and ambient gas distribution. The information we desire here, however, may be obtained by examining the behavior of α for various assumed velocity profiles.

Table 1 Dynamic efficiencies for exponential velocity profile

k	α	η
0	1.00	0.50
1	0.43	0.70
2	0.25	0.80
3	0.17	0.85
10	0.05	0.95
∞	0.00	1.00